

Dye-sensitized Solar Cell Utilizing Degussa P25 and Anatase TiO₂ films: Comparative Study of Photovoltaic Performance: Effect of N719 Dye Concentration

V.G. Maratin¹, A.M. Harun^{1,*}, M.Y.A. Rahman^{2,*}

¹ Faculty of Engineering, Universiti Malaysia Sabah, Jalan UMS, 88400, Kota Kinabalu, Sabah

² Institute of Microengineering and Nanoelectronics (IMEN), Universiti Kebangsaan Malaysia, 43600, Bangi, Selangor, Malaysia

*E-mail: mukifza@ums.edu.my (A.M. Harun); mohd.yusri@ukm.edu.my (M.Y.A. Rahman)

Received: 4 October 2019 / Accepted: 26 November 2019 / Published: 31 December 2019

This work deals with the comparison of dye-sensitized solar cell (DSSC) performance utilizing Degussa P25 and anatase TiO₂ films as photoanode of the device. The effect of N719 dye concentration on the device performance has been investigated. The concentration has been varied from 0.1 mM to 0.6 mM at 0.1 mM interval. It is found that the DSSC utilizing Degussa P25 demonstrated higher performance than that of the device with anatase TiO₂. The device utilizing Degussa P25 TiO₂ performs the highest η of 1.28% at the optimum concentration of N719 dye that is 0.4 mM. This because this device possesses the highest absorption in the visible region and lowest leak current. The device utilizing anatase TiO₂ performs the highest η of 0.447% at the optimum concentration of N719 dye that is 0.5 mM. This is due to the device has the highest absorption in the visible region, the smallest bulk and charge transfer resistance at the interface of Pt/electrolyte.

Keywords: anatase, charge transfer resistance, Degussa P25, dye-sensitized solar cell, photoanode

1. INTRODUCTION

Dye-sensitized solar cell (DSSC) is a third generation of solar cell that possesses unique characteristic feature that is much lower fabrication cost than that of conventional silicon solar cell. Nevertheless, the power conversion efficiency of the DSSC is lower than that of this first generation of solar cell due to its optical absorption in visible region is lower than that of silicon solar cell. DSSC has three important components, namely, photoanode, electrolyte and cathode. The role of photoanode in dye-sensitized solar cell (DSSC) is crucial since it accepts electrons donated by the excited dye molecules resulted from photovoltaic effect. Photoanode should possesses good electrical property such as high electronic conductivity to accept electrons from lowest unoccupied molecular orbitals (LUMO)

of dye molecules. The most common material for photoanode of DSSC is TiO_2 since this material is cheap, non-toxic, has good electrical property and high stability due to wide band gap that is 3.2 eV at room temperature [1]. TiO_2 can be prepared in film form on conducting substrates such as indium tin oxide (ITO) and fluorine tin oxide (FTO) via various techniques such as screen printing [2], spray pyrolysis [3], liquid phase deposition [4], electrophoretic deposition [5], microwave [hydrothermal [6], electrochemical anodization [7] and doctor blade [8]. However, the preparation of TiO_2 films via screen printing and doctor blade technique require TiO_2 in paste form. The paste can be prepared by grinding various types of TiO_2 powder such as P90, P25 and anatase with some organic binder such as poly(ethylene glycol) (PEG) in organic solvent such as ethanol and nitric acid such (HNO_3).

This work is concerned with the comparative study of the performance of DSSC utilizing Degussa P25 and anatase TiO_2 films. The influence of the N719 dye concentration on the performance of the device employing Degussa P25 and anatase TiO_2 coated N719 dye as photoanode has been investigated. The optical absorption of Degussa P25 and anatase TiO_2 films have been compared. The charge transfer resistance and carrier lifetime of the device employing both types of photoanode have also been compared to support the main photovoltaic parameter that is power conversion efficiency.

2. METHODOLOGY

For preparation of Degussa P25 paste, 1 ml of ethanol, 2 ml of triton-x and 0.2 ml of poly(ethylene glycol) were poured in a bottle that contain 1 g of titanium (IV) oxide. The solution was put on a hot plate and stirred using magnetic stirrer for 1 hour at room temperature at 1200 rpm. For preparation of anatase paste, 1 ml of ethanol, 2 ml of triton-x and 0.2 ml of poly(ethylene glycol) (PEG) were poured in a bottle that contain 3 g of anatase powder. Magnetic stirrer was the put inside the bottle placed on a hot plate, then stirred for 1 hour at room temperature at 1200 rpm.

For preparation of TiO_2 films, ITO substrates were firstly cleaned using acetone and ethanol in the right sequence in an ultrasonic bath. The TiO_2 layer was deposited on ITO substrates using a doctor blade technique. Degussa P25 paste was equally spread on the surface of conductive side ITO. After that, the petri dish containing the paste coated on ITOs was put on the hot plate for pre-heating process for 15 minutes at 100 °C. Next, it underwent annealing process at 400 °C for 1 hour in order to make sure the paste is strongly attached to ITO substrates. Finally, the TiO_2 films were formed. The above procedures were repeated for preparing anatase TiO_2 films. 0.1 mM of N719 dye (IUPAC name: Di-tetrabutylammonium cis-bis(isothiocyanato)bis(2,2'-bipyridyl-4,4'-dicarboxylato)ruthenium(II)) purchased from Sigma Aldrich was dissolved in ethanol as a sensitizer of TiO_2 films. The films were immersed in the dye solution for 24 hours at room temperature to ensure sufficient amount of dye molecules were adsorbed on the surface of the samples. The prepared samples were employed as the photoanode for DSSC. This procedure was then repeated for preparing 0.2, 0.3, 0.4, 0.5 and 0.6 mM N719 dye solution. Both types of TiO_2 coated N719 dye samples underwent optical absorption characterization by UV-Vis spectrometer.

The counter electrode of the device was platinum film grown on FTO substrates via sputtering technique. Redox electrolyte containing iodide/triiodide was injected into the space between TiO_2 coated N719 and platinum counter electrode. The devices with an active area of 0.23 cm² were tested in dark

and under illumination of 100 mW cm^{-2} light. The light source used was tungsten halogen lamp. The electrochemical impedance spectroscopy (EIS) under illumination of 100 mW cm^{-2} light was performed on the devices to determine the charge transport properties and carrier transport time.

3. RESULTS AND DISCUSSION

Fig. 1 shows the UV-Vis spectra of Degussa P25 TiO_2 samples coated with N719 dyes with various N719 concentrations. According to the figure, the 0.1, 0.3, 0.4 and 0.5 mM samples possess higher optical absorption in UV region (300-400 nm) than in visible region. However, the 0.2 and 0.6 mM samples display smaller absorption in UV region than in visible region. It is also noticed that all samples possess the lowest absorption in the region near infrared region (700-800 nm). Also, according to the spectra, the 0.4 mM sample has the highest absorption in the visible region, followed by 0.3, 0.5, 0.2, 0.6 and 0.1 mM, samples in the descending order.

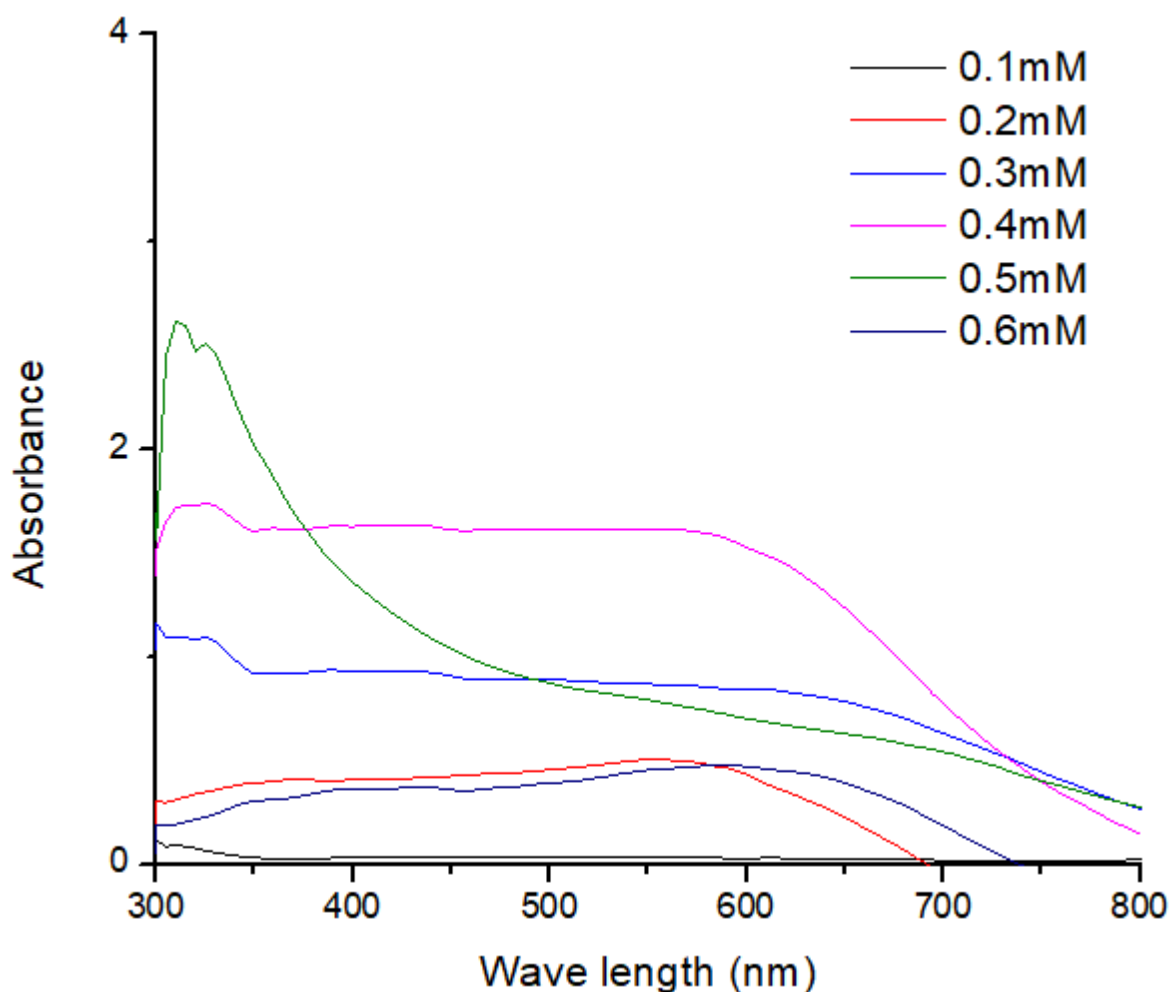


Figure 1. UV-Vis spectra of Degussa P25 TiO_2 with various N719 concentrations

Fig. 2 shows the UV-Vis spectra of anatase TiO_2 samples coated with N719 dyes with various N719 concentrations. According to the figure, the 0.1 and 0.3 mM samples possess higher optical

absorption in UV region than in visible region. However, the 0.6 mM samples display smaller absorption in UV region than in visible region. The 0.5 mM sample slightly displays higher absorption in UV than in visible region. However, the absorption of the 0.4, 0.3 and 0.2 mM samples are almost similar. It is also noticed that 0.5 and 0.6 mM samples possess the lowest absorption in the region near infrared region. Also, the 0.5 mM sample owns the highest absorption in the visible region, followed by 0.6, 0.1, and the other three samples in the descending order.

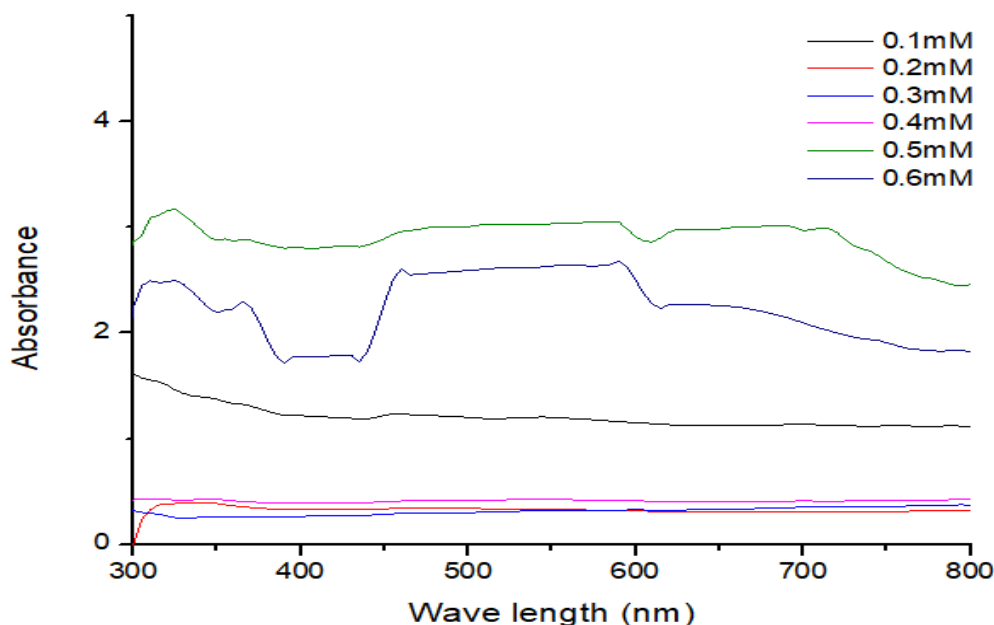


Figure 2. UV-Vis spectra of anatase TiO₂ with various N719 concentrations

Fig. 3 shows the *I-V* curves in dark of the DSSC utilizing Degussa P25 TiO₂ coated with N719 dyes with various N719 concentrations as its photoanode. According to the curves, the leak current which is also the current in reverse bias is higher than the forward current for all devices. The device utilizing the 0.2 mM sample has the highest forward current, followed by 0.3, 0.4, 0.5 and 0.6 mM samples. It is concluded that the forward current decreases with the concentration of N719 dye. While, the device utilizing the 0.5 mM sample possesses the lowest leak current, followed by 0.4, 0.6, 0.3 and 0.2 mM samples. It is observed that there is no increasing nor decreasing trend of the leak current with the concentration of N719 dye.

Fig. 4 shows the *J-V* curves under illumination of the DSSC utilizing Degussa P25 TiO₂ coated with N719 dyes with various N719 concentrations. According to the figure, the shape of the curve for the device utilizing the 0.3, 0.4 and 0.5 mM samples are almost straight line. However, the shape of the curve for the device employing the 0.1, 0.2 and 0.6 mM sample is straight line [9]. This indicates that the internal resistance in the devices is high, lowering the photocurrent in the devices. It is found that the device with the 0.4 mM sample generates the highest output power, followed by the devices with the 0.5, 0.3, 0.2 and 0.1 mM in descending order. All photovoltaics parameters are analysed from Fig. 4 and listed in Table 1.

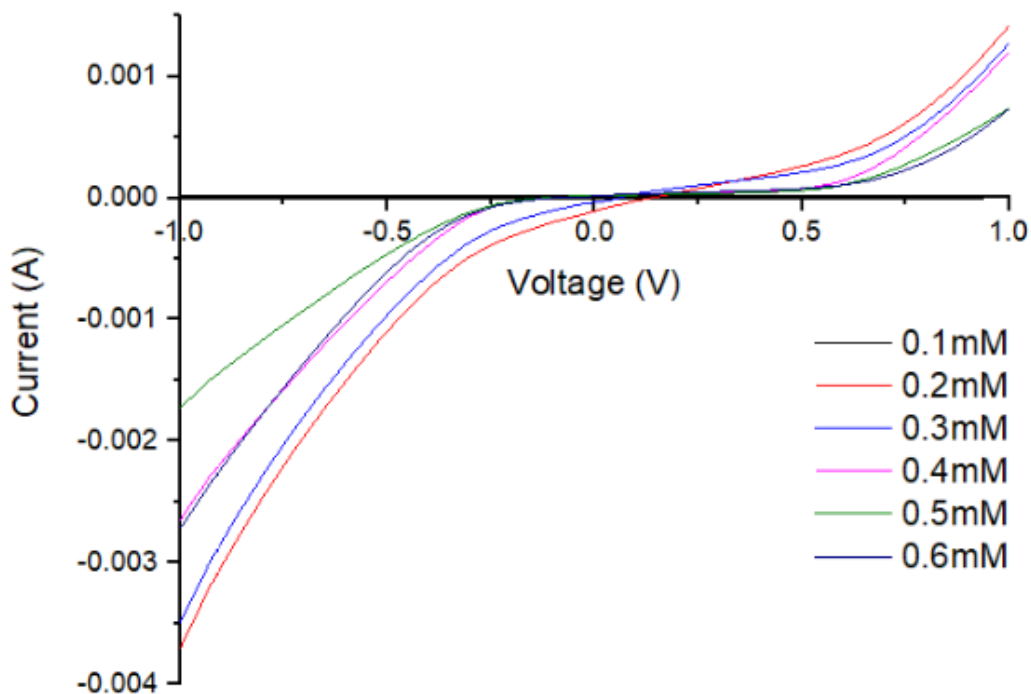


Figure 3. *I-V* curves in dark of the DSSC utilizing Degussa P25 TiO₂ with various N719 concentrations

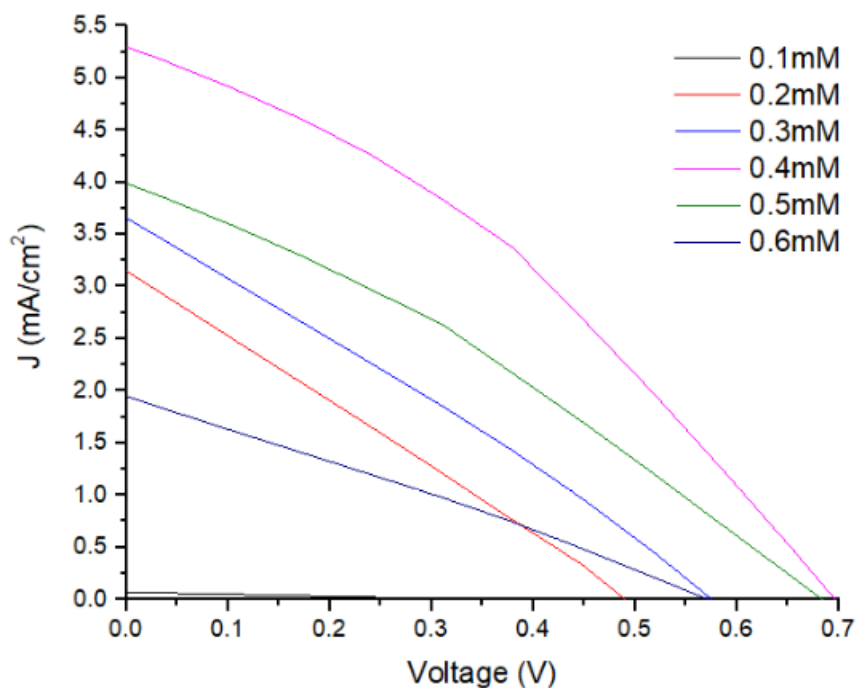


Figure 4. *J-V* curves under illumination of 100 mW cm⁻² light of the DSSC utilizing Degussa P25 TiO₂ with various N719 concentrations

Fig. 5 shows the *I-V* curves in dark of the DSSC utilizing anatase TiO₂ with various N719 concentrations. According to the curves, the leak current is higher than the forward current for all devices, similar to that of the devices using Degussa P25 TiO₂. The device utilizing the 0.6 mM sample

has the highest forward current, followed by 0.3, 0.5, 0.1, 0.2 and 0.4 mM samples. It is seen that there is no increasing nor decreasing trend of the forward current with the concentration of N719 dye. On the other hand, the device utilizing the 0.4 mM sample possesses the lowest leak current, followed by 0.2, 0.1, 0.3, 0.5 and 0.6 mM samples. It is observed that there is no increasing nor decreasing trend of the leak current with the concentration of N719 dye.

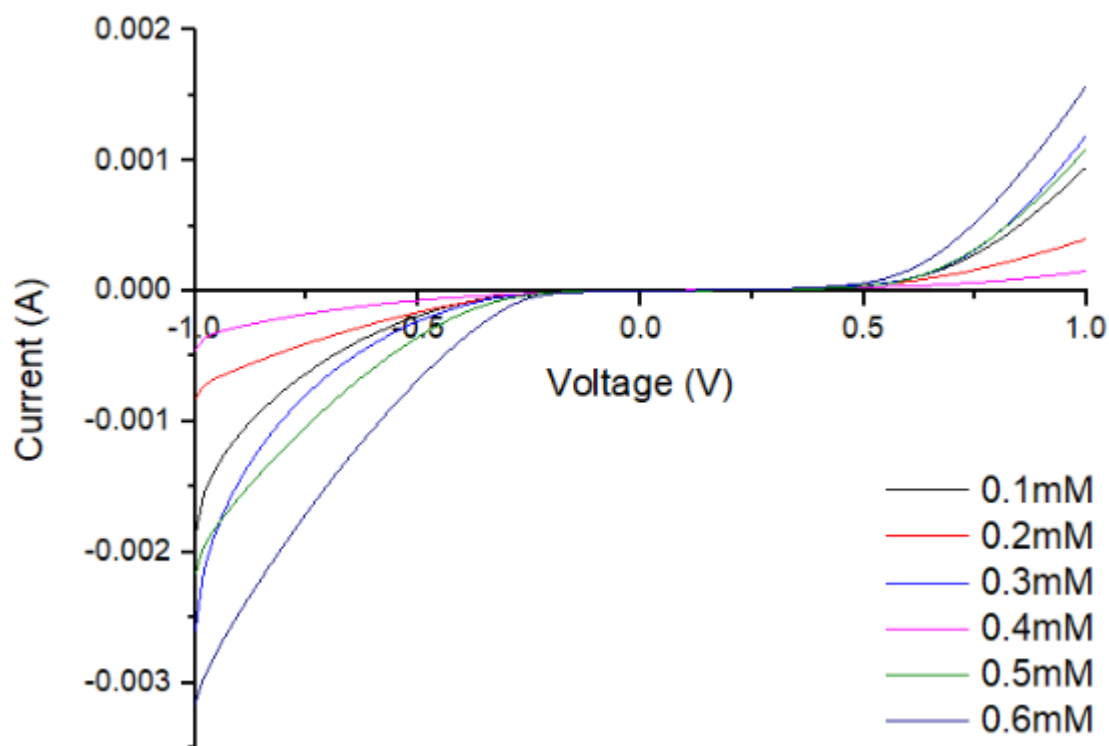


Figure 5. *I-V* curves in dark of the DSSC utilizing anatase TiO_2 with various N719 concentrations

Fig. 6 depicts the *J-V* curves under illumination of the DSSC utilizing anatase coated with N719 dyes with various N719 concentrations. According to the figure, the shape of the curve for all devices are not straight line, differ from that of the devices utilizing Degussa P25 TiO_2 . The shape is curve lines with high slope for which the current decreases quite fastly with the voltage as shown in Fig. 6 [10,11]. The internal resistance in these devices is also high, reducing the photocurrent in the devices. It is observed that the device with the 0.5 mM sample generates the highest output power, followed by the devices with the 0.6, 0.1, 0.4, 0.3 and 0.2 mM in descending order. The photovoltaics parameters are extracted from Fig. 6 and listed in Table 2.

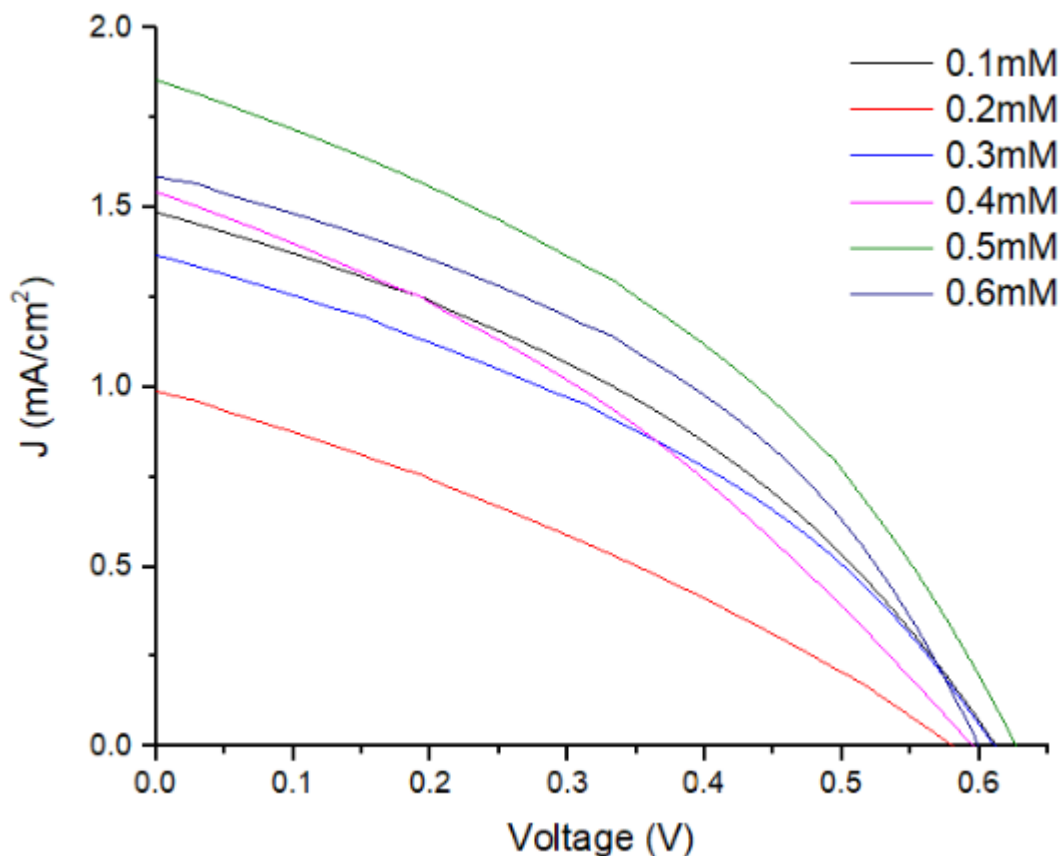


Figure 6. J - V curves under illumination of 100 mW cm^{-2} light of the DSSC utilizing anatase TiO_2 with various N719 concentrations

Fig. 7 depicts the Nyquist plots under illumination of the DSSC utilizing P25 TiO_2 with various N719 concentrations. According to the plots, there is only semicircle representing the charge transfer resistance at the interface of Pt/electrolyte (R_{ct}). While, a straight line originating from origin to starting point of the semicircle represents the bulk resistance of the device (R_b). The frequency covering the semicircle region is higher than that of straight line region. These two resistances are summarized in Table 1. It is noticeable that the R_{CT} is higher than R_b , indicating that the charge carriers moves slower at the interface of Pt/electrolyte than within the device. According to the table, it is found that the R_b and R_{ct} are high, which lowers down the J_{sc} and η which are also illustrated in Table 1. Fig. 8 displays the Bode plots under illumination of the device using P25 TiO_2 with various N719 concentrations. The plots show two peaks, however, the maximum or resonant frequency denoted by the highest peak is only used to compute the carrier lifetime (τ) and presented in Table 1. Also, according to the table, the device with 0.3 mM sample owns the lowest R_b , followed by the device with 0.1, 0.4, 0.5, 0.6 and 0.2 mM samples. The device using 0.3 mM also has the lowest R_{CT} , followed by the device using 0.2, 0.6, 0.5, 0.1 and 0.4 mM samples. Nevertheless, the value of R_{CT} for all devices is so high, affecting the photovoltaic performance of the device. For carrier lifetime, the device with 0.1 and 0.5 mM share the shortest τ followed by the 0.3, 0.4 and 0.6 mM samples which share the second shortest τ and followed by the device with 0.2 mM sample which has the longest τ .

Also, according to Table 1, the device employing the 0.04 mM sample demonstrates the highest η . However, this device does not own the smallest R_b and R_{ct} as well as the longest τ . The device with the smallest R_b , R_{ct} and the longest τ should perform the highest η . This is due to with the smaller R_{ct} , the faster reduction process taking place at the interface of Pt/electrolyte. This means the faster triiodide is reduced to iodide. This also means the faster the oxidized dye molecules to accept electrons from iodide to be regenerated to the dye molecules at ground state. The longer the carrier lifetime tells us that the slower the electrons recombine with the holes at the interface of electrolyte/TiO₂/N719 dye photoanode. The highest η owned by the device with the 0.4 mM sample can be caused by another factor such as by the highest optical absorption in the visible region as shown in Fig. 1. This is also due to the lowest leak current that this device possesses as depicted in Fig. 3. The TiO₂ coated N719 dye samples with the highest light absorption in the visible region generates the largest number of electrons from highest occupied molecular orbitals (HOMO) level to the lowest unoccupied molecular orbitals (LUMO) level. Thus, the highest number of electrons are then donated to the conduction band of TiO₂ which serves as electron acceptor. The device with the lowest leak current experiences the lowest loss of output power generated in the device. These two factors enhance the photocurrent and consequently the power conversion efficiency of the device. On the other hand, the device with 0.1 mM sample demonstrates the lowest η due to the lowest absorption in visible region.

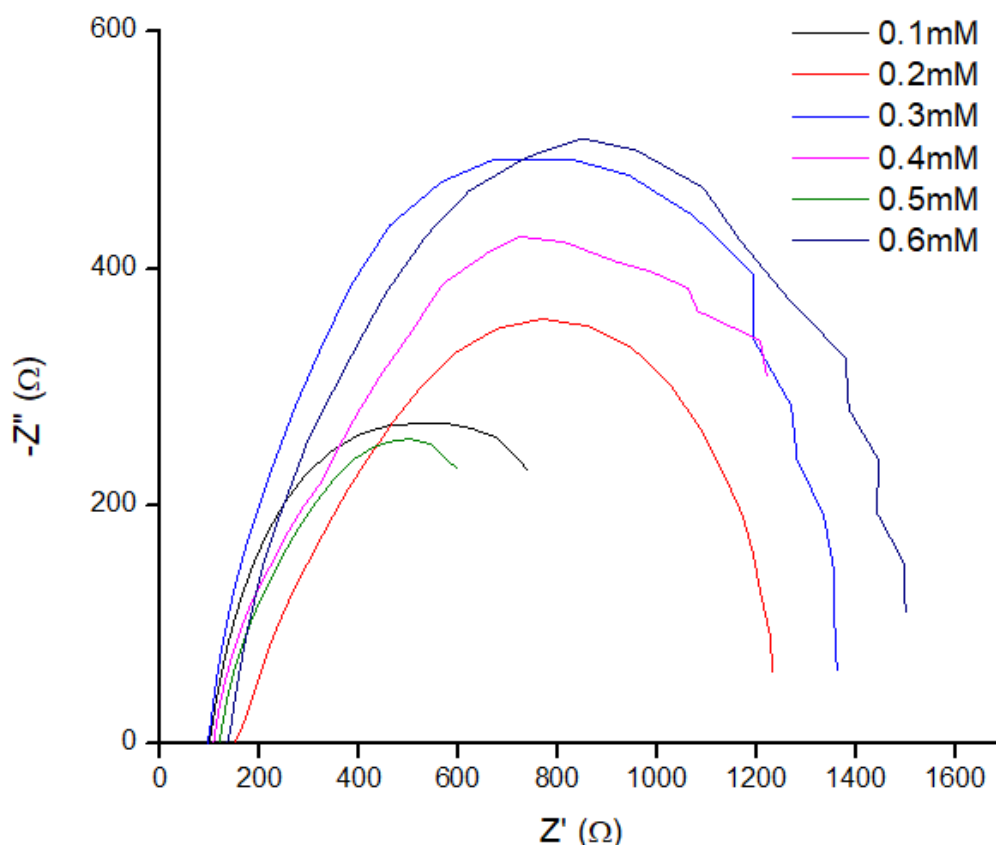


Figure 7. Nyquist plots under illumination of 100 mW cm^{-2} light of the DSSC utilizing Degussa P25 TiO₂ with various N719 concentrations

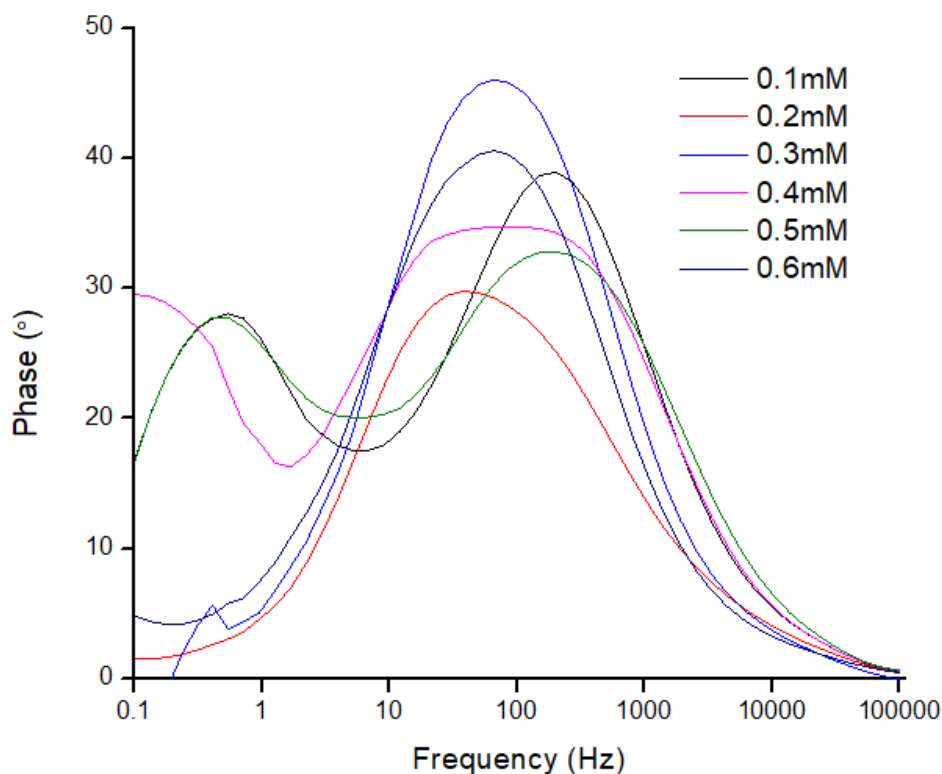


Figure 8. Bode plots under illumination of 100 mW cm^{-2} light of the DSSC utilizing Degussa P25 TiO_2 with various N719 concentrations

Table 1. Photovoltaic and EIS parameters of the DSSC utilizing Degussa P25 TiO_2 with various N719 concentrations

Molarity (mM)	V_{oc} (V)	J_{sc} (mA/cm^2)	FF	η (%)	R_b (Ω)	R_{CT} (Ω)	τ (s)
0.1	0.551	0.340	0.262	0.050	100	2395	0.0049
0.2	0.483	3.150	0.261	0.398	151	1155	0.0268
0.3	0.551	3.660	0.285	0.576	95	828	0.0153
0.4	0.689	5.300	0.351	1.280	108	2525	0.0153
0.5	0.689	3.990	0.299	0.824	121	2382	0.0049
0.6	0.551	1.950	0.283	0.304	135	1428	0.0153

Fig. 9 and 10 illustrate the Nyquist and Bode plots of the device utilizing anatase TiO_2 with various N719 concentrations, respectively. The Nyquist plot shows one semicircle and a straight line, similar to that of the Nyquist plot of the device utilizing Degussa P25. However, the Bode plots display only one peak that was then used to compute the carrier lifetime. The EIS data such as R_b , R_{CT} and τ are then summarized in Table 2. According to the table, the device with 0.5 and 0.6 mM sample own the lowest R_b , followed by the device with 0.1, 0.3, 0.2 and 0.4 mM samples. While, the device with 0.5 mM sample possesses the lowest R_{CT} , followed by 0.2, 0.6, 0.4, 0.3 and 0.1 mM samples. Also, the device using 0.5 mM sample has the shortest τ , followed by the device with 0.6, 0.2, 0.1, 0.3 and 0.4 mM samples.

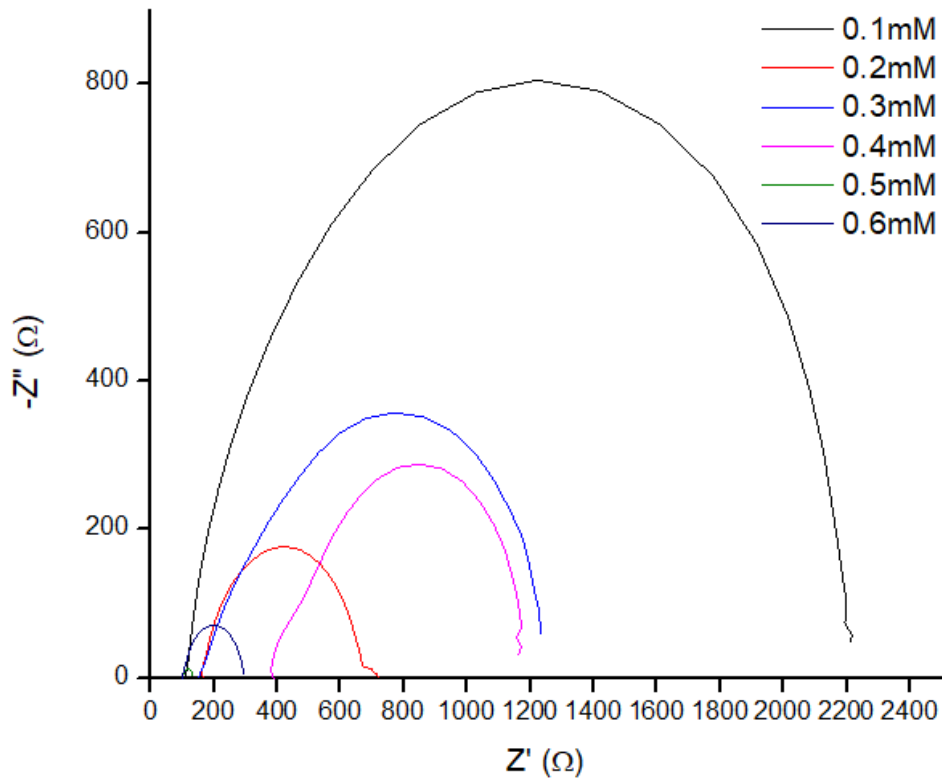


Figure 9. Nyquist plots under illumination of 100 mW cm^{-2} light of the DSSC utilizing anatase TiO_2 with various N719 concentrations

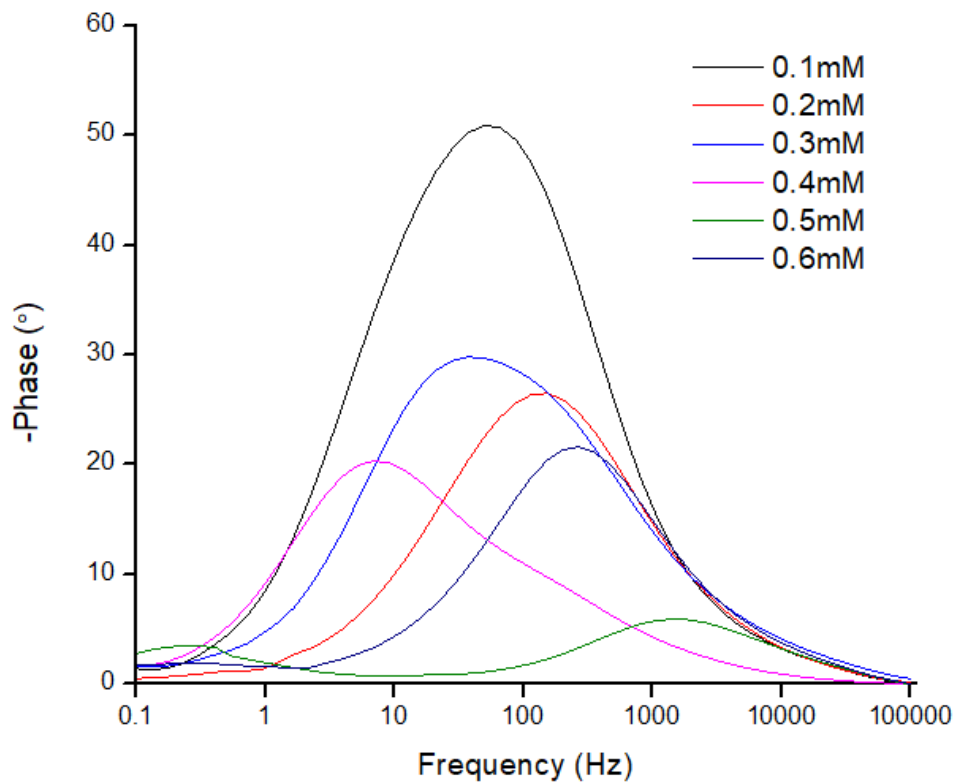


Figure 10. Bode plots under illumination of 100 mW cm^{-2} light of the DSSC utilizing anatase TiO_2 with various N719 concentrations

Table 2. Photovoltaic and EIS parameters of the DSSC utilizing anatase TiO₂ with various N719 concentrations

Molarity (mM)	V _{oc} (V)	J _{sc} (mA/cm ²)	FF	η (%)	R _b (Ω)	R _{CT} (Ω)	τ(s)
0.1	0.596	1.496	0.382	0.341	110	2099	0.020
0.2	0.576	1.000	0.308	0.177	169	169	0.007
0.3	0.596	1.378	0.378	0.311	151	1155	0.027
0.4	0.576	1.556	0.349	0.312	392	769	0.146
0.5	0.616	1.868	0.389	0.447	101	45	0.0007
0.6	0.596	1.597	0.411	0.391	101	197	0.0037

It is noticed that from Table 2, the device utilizing 0.5 mM sample demonstrates the highest η . This is due to this device has the lowest R_b and R_{CT} as shown in Table 2. Also, this is due to the device possesses the highest optical absorption in as shown in Fig. 2. The device with 0.2 mM sample performs the lowest η due to the lowest absorption in visible region.

The highest η of the DSSC employing Degussa P25 TiO₂ from this work is 1.28%. It is slightly lower than that reported in [12-14] that were 5.66, 10.1 and 4.5%, respectively. This is because the R_b and R_{CT} of the device in this work is higher than those reported in [12,13,14]. However, it is comparable with that reported in our previous work that was 1.36% [11]. While, the highest η of the DSSC employing anatase TiO₂ from this work is only 0.447%. It is much smaller than that reported in [15,16,17] that were 7.47, 7.54 and 3.0%, respectively. This is due to the R_b and R_{CT} of the device fabricated in this work are much higher than those fabricated in [15-17].

4. CONCLUSIONS

The effect of N719 dye concentration on the DSSC performance employing Degussa P25 and anatase TiO₂, respectively has been compared. It is found that the DSSC utilizing Degussa P25 demonstrated higher efficiency than that of the device with anatase TiO₂. The device utilizing Degussa P25 TiO₂ performs the highest η of 1.28% at the 0.4 mM N719 dye due to it possesses the highest absorption in the visible region and lowest leak current. The device using anatase TiO₂ performs the highest η of 0.447% at the 0.5 mM N719 dye due to the device owns the highest absorption in the visible region, the smallest bulk and charge transfer resistance at the interface of Pt/electrolyte.

ACKNOWLEDGEMENTS

The authors would like to thank UKM for providing financial assistance under a research grant FRGS/1/2019/STG02/UKM/02/1 and GUP-2018-081 for carrying out this work.

References

1. S.N. Sadikin, M.Y.A. Rahman and A.A. Umar, *Superlatt. Microstruc.*, 130 (2019) 153.
2. M.Y.A. Rahman, M.M. Salleh, I.A. Talib and M. Yahaya, *Curr. App. Phys.*, 5 (2005) 599.
3. S. Zhang, Y.F. Zhu and D.E. Brodie, *Thin Solid Films*, 213 (1992) 265.

4. A.A. Umar, M.Y.A. Rahman, S.K.M. Saad, M.M. Salleh and M. Oyama, *App. Surf. Sci.*, 270 (2013) 109.
5. M. Zhou, J. Yu, S. Liu and P. Zhai, *J. Hazard. Mater.*, 154 (2008) 1141.
6. S Pushpakanth, B Srinivasan, B Sreedhar and T.P. Sastry, *Mater. Chem. Phys.*, 107 (2008) 492.
7. Y. Tang, J. Tao, Y. Zhang, T. Wu, H. Tao and Z. Bao, *Acta Phy-Chim. Sinica*, 24 (2008) 2191.
8. N.N. Dinh, N.M. Quyen, D.N. Chung, M. Zikova and V.V. Truong, *Sol. Energy Mater. Sol. Cells*, 95 (2011) 618.
9. M.Y.A. Rahman, M.M. Salleh, I.A. Talib, M. Yahaya and A. Ahmad, *Curr. App. Phys.*, 7 (2007) 446.
10. S.A.M. Samsuri, M.Y.A. Rahmana and A.A. Umar, M.M. Salleh, *Mater. Lett.*, 160 (2015) 388.
11. M.Y.A. Rahman, L. Roza, S.A.M. Samsuri and A.A. Umar, *Russ. J. Electrochem.*, 54 (2018) 755.
12. D. Chen, F. Huang, Y.B. Cheng and R.A. Caruso, *Adv. Mater.*, 21 (2009) 2206.
13. Y. Yasuhiro, K. Masahide, S. Hiroshi, U. Satoshi, K. Junya, S. Fumio, T. Kazuki, S. Tsubasa and I. Seigo, *Chem. Lett.*, 40 (2011) 1220.
14. V. Dhas, S. Muduli, S. Agarkar, A. Rana, B. Hannoyer, R. Banerjee and S. Ogale, *Sol. Energy*, 85 (2011) 1213.
15. X. Wu, Z. Chen, G.Q. Lu and L. Wang, *Adv. Funct. Mater.*, 21 (2011) 4167.
16. H.G. Jung, Y.S. Kang and Y.K. Sun, *Electrochim. Acta*, 55 (2010) 4637.
17. A.A. Umar, S. Nafisah, S.K.M. Saad, S.T. Tan, A. Balouch, M.M. Salleh and M. Oyama, *Sol. Energy Mater. Sol. Cells*, 122 (2014) 174.

© 2020 The Authors. Published by ESG (www.electrochemsci.org). This article is an open access article distributed under the terms and conditions of the Creative Commons Attribution license (<http://creativecommons.org/licenses/by/4.0/>).